# FRET-Based Nanoscale Point-to-Point and Broadcast Communications With Multi-Exciton Transmission and Channel Routing

Murat Kuscu*, *Student Member, IEEE*, and Ozgur B. Akan, *Senior Member, IEEE*

***Abstract*—Nanoscale communication based on Förster Resonance Energy Transfer (FRET) enables nanoscale single molecular devices to communicate with each other utilizing excitons generated on fluorescent molecules as information carriers. Based on the point-to-point single-exciton FRET-based nanocommunication model, we investigate the multiple-exciton case for point-to-point and broadcast communications following an information theoretical approach and conducting simulations through Monte Carlo approach. We demonstrate that the multi-exciton transmission significantly improves the channel reliability and the range of the communication up to tens of nanometers for immobile nanonodes providing high data transmission rates. Furthermore, our analyses indicate that multi-exciton transmission enables broadcasting of information from a transmitter nanonode to many receiver nanonodes pointing out the potential of FRET-based communication to extend over nanonetworks. In this study, we also propose electrically and chemically controllable routing mechanisms exploiting the strong dependence of FRET rate on spectral and spatial characteristics of fluorescent molecules. We show that the proposed routing mechanisms enable the remote control of information flow in FRET-based nanonetworks. The high transmission rates obtained by multi-exciton scheme for point-to-point and broadcast communications, as well as the routing opportunities make FRET-based communication promising for future molecular computers.**

***Index Terms*—FRET, nanoscale communications, nanonetworks, broadcast networks, routing, channel capacity, ISI, error probability, transmission rate, fluorescent molecules, QCSE, interlocked molecules.**

## I. Introduction

NANOTECHNOLOGY has enabled manufacturing of nano-size machines which are capable of performing simple actuating, sensing and computing tasks. A number of nanomachines communicating with each other is envisioned as a *nanonetwork*. Nanonetworks allow nanomachines to cooperatively exchange information to achieve more complex tasks ranging from nuclear defense to in-body drug delivery and disease treatments [1]. The exchanged information among nanomachines might be an output of a sensing process or a logic operation, as well as a control signal sent by a remote information source that intends to control the operation of nanomachines. Modeling the potential information sharing mechanisms among nanomachines and investigating the methods for controlling the route of the information flow at nanoscale are crucial for the design of fully functional nanomachines with networking capabilities. Several approaches have been proposed in order to achieve communication at nanoscale such as electromagnetic, acoustic, nanomechanical or molecular, some of which are inspired by nature [2], [3]. In addition to the existing techniques, recently, we have proposed and investigated a novel and radically different nanoscale molecular communication method exploiting a well-known phenomenon FRET [4].

FRET is a pairwise non-radiative energy transfer process observed among fluorescent molecules, i.e., fluorophores, such as organic dyes, fluorescent proteins, as well as semiconductor nanoparticles, e.g., Quantum Dots (QDs), which have spectral similarities, and are located in a close proximity such as 0–10 nm [9]. The phenomenon has been widely used in studies of biotechnological research including fluorescence microscopy, molecular biology, and optical imaging, since it provides a significant amount of structural and spatial information about molecules by means of optical signals with nanoscale resolution [10], [11]. Several chemical and biological nanosensors based on FRET, some of which utilize DNA as the scaffold for fluorophores, have been developed [12], [13]. Furthermore in nanomedicine, exploiting FRET, QDs have been employed as the photosensitizing agents for photodynamic therapy (PDT) in cancer treatment [14], [15]. Moreover, the quantum coherence behavior of FRET in short distances has been widely studied showing the potential usage of FRET for future quantum computer designs [16].

Using FRET as a communication mechanism for single-molecular nanonodes has been first proposed in [4]. In that study, we have modeled point-to-point and multi-step FRET-based communication channels between immobile single-molecular nanonodes, and analyzed their information theoretical capacity for varying internal and environmental parameters. In that basic model, communication between nanonodes was realized via the transfer of single excited

Manuscript received April 12, 2013; revised May 24, 2014; accepted July 07, 2014. Date of publication July 30, 2014; date of current version September 23, 2014. This work was supported in part by the Turkish Scientific and Technical Research Councilunder Grant #109E257, by the Turkish National Academy of Sciences Distinguished Young Scientist Award Program (TUBA-GEBIP), and by IBM through IBM Faculty Award. An earlier version of this work was presented at IEEE MoNaCom'12, Ottawa, Canada. *Asterisk indicates corresponding author.*

*M. Kuscu is with the Next-generation and Wireless Communications Laboratory (NWCL), Department of Electrical and Electronics Engineering, Koc University, Istanbul, 34450, Turkey (e-mail: mkuscu, akan@ku.edu.tr).

O. B. Akan is with the Next-generation and Wireless Communications Laboratory (NWCL), Department of Electrical and Electronics Engineering, Koc University, Istanbul, 34450, Turkey (e-mail: mkuscu, akan@ku.edu.tr).

Color versions of one or more of the figures in this paper are available online at http://ieeexplore.ieee.org.

Digital Object Identifier 10.1109/TNB.2014.2342712

state, i.e., single exciton, generated by a remote information source (IS) on a donor fluorophore acting as the Transmitter Nanonode (TN) to an acceptor fluorophore acting as the Receiver Nanonode (RN). It has been shown that FRET-based nanoscale communication outperforms the other short range communication methods in terms of reliability and communication rate as well as controllability. We also investigated the multi-step FRET-based long-range nanocommunication channel [5], FRET-based mobile molecular ad hoc nanonetworks [6], [7], and graphene plasmon-assisted FRET-based nanocommunication channel [8] to derive their information theoretical models, and evaluate the communication performance.

In this study, based on the channel model given in [4], we investigate the feasibility and performance of FRET-based broadcast communication channel between one TN and many RNs from the network perspective. Furthermore, exploiting Quantum Confined Stark Effect (QCSE) observed in semiconductor nanoparticles, we propose an electrically controllable routing mechanism for FRET-based nanonetworks. In this paper, we also extend our preliminary work in [17]. Differing from our previous work, we propose encoding information into multiple excitons, instead of single-excitons, in order to improve the reliability of the communication. We analyze the performance of FRET-based point-to-point and broadcast communication channels with multi-exciton transmission. Additionally, we propose another chemically controllable routing method based on the nanoscale shuttle-like movement of [2]rotaxane macrocycle between two nodes with acid/base treatment. We conclude that information flow can be directed in an FRET-based nanonetwork by either external control, i.e., electric field, or depending on environmental conditions, i.e., acid/base condition. Performance evaluations of the communication channels and routing methods are carried out through simulations with Monte Carlo algorithms based on the competitive behavior of multiple excitons.

The remainder of this paper is organized as follows. In Section II, we briefly review the basics of FRET and FRET-based nanoscale communications. In Section III, we model FRET-based point-to-point and broadcast communication channels with multi-exciton transmission. The electrical and chemical routing mechanisms for FRET-based nanonetworks are proposed and investigated in Section IV. In Section V, we evaluate the performance of the proposed communication and routing schemes by means of information theoretical capacity. Finally, the concluding remarks are given in Section VI.

## II. Background

### A. FRET Theory

FRET defines the non-radiative energy transfer from a donor molecule (D) to a proximal acceptor molecule (A). It is observed among the fluorescent molecules with chromophore units that are able to be excited by optical, electrical or chemical energy at a specific range of wavelength and emit that absorbed energy at a different wavelength.

Theodor Förster postulated the governing equations of FRET theory in his seminal work [18]. The main equations are then validated experimentally [11]. As Förster stated, there are mainly two requirements for FRET to occur between two molecules; spectral similarity and proximity [18]. The spectral characteristics of donor and acceptor must have significant similarity, i.e., the overlapping area of the emission spectrum of the donor and the absorption spectrum of the acceptor must be large enough. The spectral similarity is proportional to the resonance probability of the molecule transition dipoles. In addition, the molecules must be in a close proximity such as 0–10 nm. When these conditions are satisfied, FRET competes with fluorescence process. The probability of FRET can be given in terms of process rates as

$$P_{\mathrm{FRET}} = \frac{k_T}{k_R + k_T} \tag{1}$$

where $k_R$ and $k_T$ are the fluorescence and FRET rates, respectively. $k_R$ is the reciprocal of the mean of excited state lifetime of the donor $\tau_D$ in the absence of a nearby acceptor, i.e., $1/\mu_{\tau_D}$. $\tau_D$ denotes the time that the excited donor molecule stays in the excited state before relaxing through fluorescence, and it is an exponential random variable [9]. The mean lifetime is shortened when there exists different pathways for the donor to relax including FRET. In case there exists an acceptor in the proximity of the donor, the mean of the donor lifetime $\tau_{DA}$ is given as

$$\mu_{\tau_{DA}} = \frac{1}{k_R + k_T} \tag{2}$$

$\tau_{DA}$ is also an exponential random variable [9]. FRET rate $k_T$ is given in terms of fluorescence rate as

$$k_T = k_R \left( \frac{R_0}{R} \right)^6 \tag{3}$$

where $R_0$ is the Förster radius denoting the distance between the molecules when $P_{\mathrm{FRET}}$ is 0.5, and $R$ defines the intermolecular distance between the transition dipole centers of the molecules. $R_0$ relates the FRET rate with environmental and intrinsic parameters and can be expressed by

$$R_0^6 = 8.8 \times 10^{22} \kappa^2 n^{-4} Q_D \int_0^\infty F_D(\lambda) \epsilon_A(\lambda) \lambda^4 \mathrm{d}\lambda \tag{4}$$

where $\kappa^2$ is the relative orientation factor, $Q_D$ is the quantum yield of the donor, and $n$ is the refractive index of the medium. The integral part of (4) denotes the degree of the overlap of the donor emission spectrum and the acceptor absorption spectrum, and is denoted by $J(\lambda)$,

$$J(\lambda) = \int_0^\infty f_D(\lambda) \epsilon_A(\lambda) \lambda^4 \mathrm{d}\lambda \tag{5}$$

where $f_D(\lambda)$ is the normalized fluorescence emission intensity, and $\epsilon_A(\lambda)$ is the acceptor molar absorptivity. The orientation factor $(\kappa^2)$ can be given as

$$\kappa^2 = (\cos\theta_T - 3\cos\theta_D \cos\theta_A)^2 \tag{6}$$

where $\theta_T$, $\theta_D$ and $\theta_A$ are the angles determined by the emission and absorption transition dipoles of the fluorophores [9]

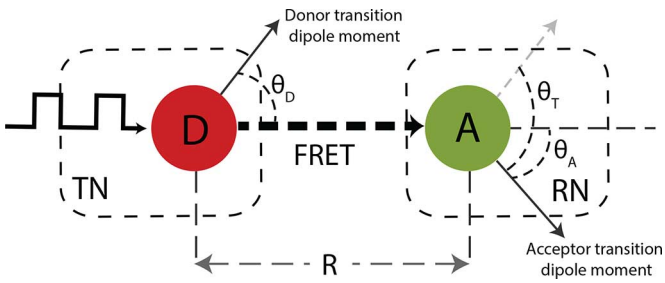


Fig. 1. Point-to-point FRET-based nanocommunication channel model.

as shown in Fig. 1. Assuming isotropic and unrestricted distributions for all three angles, the distribution of $\kappa^2$ can be given as [19]

$$p_{\kappa^2}(\kappa^2) = \begin{cases} \frac{1}{2\sqrt{3\kappa^2}} \ln\left(2+\sqrt{3}\right) & 0 \le \kappa^2 \le 1 \\ \frac{1}{2\sqrt{3\kappa^2}} \ln\left(\frac{2+\sqrt{3}}{\sqrt{\kappa^2}+\sqrt{\kappa^2-1}}\right) & 1 \le \kappa^2 \le 4 \end{cases} \tag{7}$$

Due to the strong dependence of the transfer efficiency on the spatial parameters of the participating molecules, FRET is widely exploited as an experimental tool in biotechnological research to observe the molecular events of conformation, association, separation and diffusion. There are numerous methods to exploit FRET in fluorescence microscopy such as fluorescence-detected excited state lifetime (FLIM), bioluminescence RET (BRET), and photobleaching FRET (pbFRET) [10]. Among these methods, single-molecule FRET (smFRET), which defines the use of single pair of donor and acceptor for microscopic observations, is continuously being advanced parallel to the developments in nanotechnology and gaining increased popularity, since it provides radically higher temporal and spatial resolution compared to the bulk solution FRET methods. Recently, smFRET has been proposed to increase the spatial resolution and sensitivity of apertured Scanning Near-field Optical Microscopy (SNOM) which is limited by the size of the aperture for light transmission, e.g., a typical value of 50 nm [21]. In the same study, the first microscopic images with a spatial resolution of the order of Förster radius were obtained using smFRET SNOM.

### *B. FRET-Based Nanoscale Communications*

The point-to-point FRET-based nanoscale communication system proposed in [4] consists of three main parts; a Transmitter Nanonode (TN) which is a single donor fluorophore, a communication channel, and a Receiver Nanonode (RN) which is a single acceptor fluorophore.

The system utilizes a pulsed laser as IS that can generate picosecond-duration excitation pulses, and implements ON-OFF keying (OOK) modulation with two bits available; bit-0 and bit-1. When IS intends to transfer bit-1, a single laser pulse which has a wavelength near to the excitation maximum of the donor is sent to TN at the beginning of a fixed-duration time slot. The donor fluorophore acting as TN is excited by this pulse and after some time it relaxes through either fluorescence or FRET by transferring its excited energy to a nearby acceptor fluorophore, i.e., RN, and making the acceptor excited. If FRET occurs following the excitation of the donor, RN detects bit-1. In the bit-0 case, IS does not send any pulse to TN and keeps it silent in a time slot duration. Therefore, RN also stays in the ground state, detects bit-0. The time slot determines the bit interval, i.e., bit period, $T_b$.

A fluorophore in its excited state cannot be re-excited until it relaxes to the ground state [9]. If slot durations are not arranged properly, this fact results in InterSymbol Interference (ISI) such that when IS sends successive bit-1's to TN, some of the bits cannot be transmitted through the channel if the donor or acceptor is in the excited state due to the preceding bit-1 transmission. We have to consider the worst-case in determining the minimum bit interval $T_{b-\min}$, i.e., minimum slot duration, required to avoid ISI. In the worst case, the exciton generated by IS stays on the donor for time $\tau_{DA,\max}$, and then it is transferred to the acceptor where it stays for time $\tau_{A,\max}$. Here, $\tau_{DA,\max}$ and $\tau_{A,\max}$ are the maximum donor lifetime in the presence of a nearby acceptor, and the maximum acceptor lifetime, respectively. After a time of $\tau_{DA,\max}+\tau_{A,\max}$, the exciton is removed from the system. Therefore, $T_{b-\min}$ is expressed as follows

$$T_{b-\min} = \tau_{DA,\max} + \tau_{A,\max} \tag{8}$$

Since the molecule lifetimes are modeled as exponential random variables, setting $T_b$ equal to $4 \times (\mu_{\tau_{DA}} + \mu_{\tau_A})$ results in an ISI probability below $10^{-3}$ that might be enough to neglect ISI in some cases.

If the bit interval satisfies the no-ISI criteria, assuming that the donor is guaranteed to be excited by each laser pulse, and neglecting the direct excitation of the acceptor by the laser pulse, the successful transmission probability of bit-1, i.e., $p_1$, is equal to $P_{\mathrm{FRET}}$. Assuming there is no another excitation source that can excite the acceptor independently, the successful transmission probability of bit-0 is equal to 1. Therefore, the channel is modeled information theoretically as a Z-channel.

Using fluorescent molecules at the single molecular level, i.e., without a bulk solution, for FRET-based communications brings some crucial challenges originated from the photochemical properties of the molecules. Fluorescent molecules undergo photochemical destruction and lose their fluorescence ability after a number of excitation-relaxation cycles under illumination. Their resistance to the photobleaching event, which depends on the intrinsic molecular characteristics, the excitation wavelength and intensity, determines their photostability [9]. Therefore, photostability of the employed single molecules acting as communication nodes is one important parameter setting a limit for the lifetime of the whole system.

Dye molecules are extensively used in fluorescence microscopy, and thus, their photochemical and spectral characteristics are well-known. As most of the theoretical FRET-based studies, we based our work on the properties of widely-used organic dyes, to derive the theoretical framework, and basically evaluate the communication performance. However, we know that most of the dye molecules are not sufficiently photostable and undergo photobleaching after $\sim 10^5 - 10^6$ excitation/relaxation cycles [9], therefore, it may lead to feasibility problems

for FRET-based communications depending on the application. To establish communications for the applications requiring long-time operability, more stable fluorescent molecules need to be employed. Semiconductor QDs with inorganic surface layers shielding the core material are proved to be 100 times more stable than conventional organic dyes [22], and find increasing number of applications in fluorescence microscopy including FRET-based imaging techniques. However, QDs suffer from photoblinking, i.e., photoluminescence intermittency, and their toxicity limits their usage for in vivo applications [9]. Recently, Nitrogen-Vacancy (NV) centers in nanodiamonds have been proposed as highly-stable local fluorescence probes with nearly infinite lifetime and proved to be suitable for FRET-based applications including quantum information processing [23]. Therefore, they may provide more convenient alternative to organic dyes and QDs to overcome the photostability problem for FRET-based communications.

## III. Multi-Exciton Transmission

FRET-based communication can be very unreliable if the internodal distance is greater than the Förster radius of the molecules [4], or there are more than one RN communicating with TN. In order to reduce the error probability, one might come up with the idea of transmitting the signal many times through the channel. However, without a feedback mechanism, i.e., without the knowledge of the TN about the success of the transmission, this method has to be applied for each transmission with the number of repetitions determined prior to communication. For the case of single pair TN-RN communication with fixed repetitions, the bit interval required for negligible ISI is multiplied with the number of repetitions, $N$:

$$T_{b,\mathrm{repeat-min}} = N \times T_{b,\min} = N \times (\tau_{DA,\max} + \tau_{A,\max}) \quad (9)$$

Assuming, $R, m$, and $\kappa^2$ are constant for each transmission, the transmission probability of bit-1 becomes

$$p_1 = 1 - (1 - P_{\mathrm{FRET}})^N \quad (10)$$

$p_0$ is again equal to 1 for repeated transmission. As can be seen intuitively, this transmission scheme significantly reduces the error probability of bit-1. Therefore, the capacity is expected to increase with increasing $N$. However, high bit duration $T_b$ required for negligible ISI significantly reduces the transmission rate.

Since the excited state lifetimes of the molecules are random variables with exponential distributions, it is very possible for an exciton to be removed from the system in a duration smaller than $T_{b,\min}$. This makes it inefficient for IS to send fixed period pulses to TN. An alternative way to reduce the error probability of transmission with relatively small bit intervals is to increase the pulse duration sent by IS into nanoseconds range and allow many excitations to be generated on TN in one pulse duration with a probabilistic manner. In this scheme, for the representation of bit-1, IS continuously sends photons or electrons to TN in a pulse duration. TN is expected to be excited by the first photon or electron coming from IS. After a duration of $\tau_{DA}$, TN relaxes through FRET or fluorescence. If $\tau_{DA}$ is smaller than the pulse duration, then TN is excited again as soon as it relaxes, and this continues until the pulse duration ends. In other words, multiple excitons are transmitted during a pulse duration to represent bit-1.

In the following sections, multi-exciton transmission scheme is applied to FRET-based point-to-point and broadcast channels; and we obtain the channel capacities through Monte Carlo simulations.

### A. FRET-Based Point-to-Point Communication With Multi-Exciton Transmission

In this section, we revisit our point-to-point communication channel model in order to investigate the communication performance of the channel with multi-exciton transmission scheme. Here, IS sends an optical or electrical pulse with $T_{\mathrm{pulse}}$ duration to TN in the beginning of a $T_b$-duration time slot to make it transmit bit-1. In order for TN to transmit bit-0, IS does not send any pulse during the time interval $T_b$. In one slot time interval, i.e., bit interval, TN can be excited and relaxed through FRET or fluorescence many times. When RN is excited through FRET, bit-1 is detected by RN, and then the transferred exciton is removed from the system after a random occupation time, $\tau_A$, which is also an exponential random variable with mean $\mu_{\tau_A}$. Once RN detects bit-1, it neglects other excitations until the current bit interval ends. If RN is not excited in a bit duration, it decides that bit-0 is sent.

Assuming that there is no other excitation source except IS, the successful transmission probability of bit-0, i.e., $p_0$, equals to 1. The transmission probability of bit-1 can be written as

$$p_1 = 1 - \prod_{i=1}^{N} (1 - P_{\mathrm{FRET},i}) \quad (11)$$

where $N$ is a random variable which defines the number of excitons generated by the pulse with duration $T_{\mathrm{pulse}}$. Note that in this scheme, TN is always in the excited state during $T_{\mathrm{pulse}}$, such that, when it is relaxed through fluorescence or FRET, it is immediately excited by another photon or electron coming from IS. Therefore, the generation time of the $i$th exciton on the donor is expressed by

$$T_{g,i} = \sum_{l=1}^{i-1} \tau_{DA,l} \quad (12)$$

where $\tau_{DA,i}$ denotes the excited state lifetime of the donor for the $i$th exciton, i.e., the occupation time of the $i$th exciton on the donor. $\tau_{DA,i}$ is an exponential random variable with a mean that depends on the state of the acceptor at time $T_{g,i}$. The acceptor can be in the excited state at time $T_{g,i}$ due to the transfer of a preceding exciton. Therefore, $\mu_{\tau_{DA,i}}$ can be expressed as

$$\mu_{\tau_{DA,i}} = \begin{cases} \frac{1}{k_R} & \text{if A is excited at } T_{g,i} \\ \frac{1}{k_R + k_{T,i}} & \text{if A is available at } T_{g,i} \end{cases} \quad (13)$$

where $k_{T,i}$ is the FRET rate for the $i$th exciton that can be given as follows

$$k_{T,i} = k_R \left( \frac{R_{0,i}}{R} \right)^6 \quad (14)$$

where $R_{0,i} = (8.8 \times 10^{22}\kappa_i^2 n^{-4} J(\lambda))^{1/6}$. $R_{0,i}$ depends on the random variable $\kappa_i^2$ which defines the relative orientation of the fluorophores during the generation and relaxation of the $i$th exciton. Assuming that molecules are isotropically free, $\kappa_1^2, \ldots, \kappa_N^2$ are independent and identically distributed (i.i.d.) random variables with the probability distribution defined in (7).

Accordingly, the $i$th exciton on the donor fluoresces or is transferred to the acceptor through FRET at time $T_{r,i} = T_{g,i} + \tau_{DA,i}$. If the exciton is transferred to the acceptor at $T_{r,i}$, it occupies the acceptor until the acceptor fluoresces at time $T_{r,i} + \tau_{A,i}$. Note that the emission spectrum of the acceptor and the absorption spectrum of donor are assumed to be non-overlapping, therefore, fluorescence is the only way for the excited acceptor to relax. $\tau_{A,i}$ denotes the occupation time of the $i$th exciton on the acceptor, and it is an exponential random variable with mean $\mu_{\tau_A}$. The exciton $i$, stays in the system for $\tau_{DA,i}$, if it results in fluorescence of the donor; and for $\tau_{DA,i} + \tau_{A,i}$, if it results in fluorescence of the acceptor.

The FRET probability for the $i$th exciton, i.e., $P_{\mathrm{FRET},i}$, is a random variable that depends on the state of the acceptor at time $T_{r,i}$:

$$P_{\mathrm{FRET},i} = \begin{cases} 0 & \text{if A is excited at } T_{r,i} \\ \frac{k_{T,i}}{k_R + k_{T,i}} & \text{if A is available at } T_{r,i} \end{cases} \quad (15)$$

The randomness of $P_{\mathrm{FRET},i}$ and $p_1$ is originated from the random nature of relative orientations and occupation times. Due to high degree of stochasticity, we simulate the transmission of bit-1 following a Monte Carlo approach to obtain numerical expressions for $p_1$ and ISI probability. Using the obtained values, we analyze the channel capacity and achievable rates in Section V-A.

### *B. FRET-Based Broadcast Communication With Multi-Exciton Transmission*

FRET occurs when the transition dipole moments of two fluorophores come into resonance. Therefore, FRET is a pairwise energy transfer, such that it is not possible for an excited donor molecule to transfer its excited energy to more than one acceptors at the same time. However, if the donor is excited and relaxed continuously for a sufficiently large time interval, as in the case of multi-exciton transmission, it is possible that each of the acceptor molecules is excited through FRET by different excitons.

FRET-based broadcast communication can be realized with one TN surrounded by many RNs in a close proximity as seen in Fig. 2. TN sends the same binary information come from IS to each of RNs. The information theoretical capacity of this broadcast communication channel is limited by the performance of the worst point-to-point channel in the network. If we assume that RNs are located by the same distance from TN, the broadcast channel capacity equals to the capacity of one of the TN-RN point-to-point channels. Therefore, we investigate the binary transmission probabilities through single TN-RN channel in the broadcast network to determine the overall broadcast channel capacity.

Assuming that TN communicates with $k$ number of RNs, the successful transmission probability of bit-1 to the $j$th RN, $p_{1,j}$,

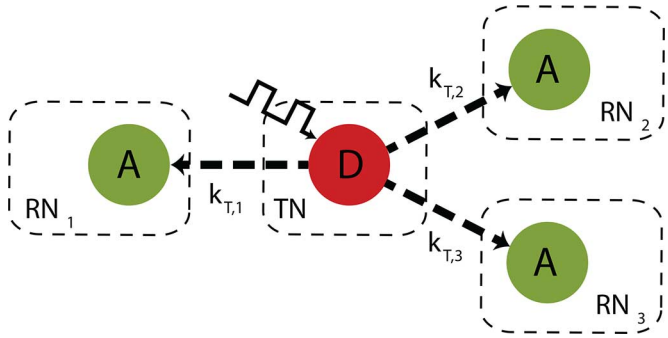


Fig. 2. Demonstration of FRET-based broadcast communication with a single TN communicating with three RNs in close proximity.

is the probability that $j$th RN gets excited via FRET in a bit interval $T_b$, when TN is continuously excited by IS in a time duration of $T_{\mathrm{pulse}}$. Note that $T_{\mathrm{pulse}} \leq T_b$, and $T_{\mathrm{pulse}}$ begins at the beginning of $T_b$. Assuming that the length of $T_b$ guarantees the no-ISI condition, $p_{1,j}$ can be given as

$$p_{1,j} = 1 - \prod_{i=1}^{N} (1 - P_{\mathrm{FRET},j,i}) \quad (16)$$

$p_{0,j}$, i.e., the non-excitation probability of the $j$th RN during $T_b$, when IS sends no pulse, is 1 assuming that there is no other excitation source. Here, $P_{\mathrm{FRET},j,i}$ is a random variable that represents the probability of FRET between TN and the $j$th RN for the $i$th exciton. $N$ is a random variable indicating the number of the excitons generated by one pulse. Note that the donor is always in the excited state, and the generation time of the $i$th exciton is given as in (12). $\tau_{DA,i}$, i.e., the occupation time of the exciton $i$ on the donor, is an exponential random variable and its mean can be expressed as

$$\mu_{\tau_{DA,i}} = \left( k_R + \sum_{j=1}^{k} k_{T,j,i} \mathbf{1}_{g,j,i} \right)^{-1} \quad (17)$$

where $k_{T,j,i}$ is a random variable which defines the FRET rate between TN and the $j$th RN for the $i$th exciton, and $\mathbf{1}_{g,j,i}$ is the indicator function defined on the set of the acceptor molecules. $\mathbf{1}_{g,j,i} = 1$, if the $j$th acceptor $A_j$ is available at time $T_{g,i}$, and $\mathbf{1}_{g,j,i} = 0$, if $A_j$ is in the excited state at time $T_{g,i}$. $k_{T,j,i}$ in terms of the orientation parameter can be expressed by

$$k_{T,j,i} = 8.8 \times 10^{22} \kappa_{j,i}^2 n^{-4} J_j(\lambda) \frac{k_R}{R_j^6} \quad (18)$$

where $R_j$ is the distance between the centers of the transition dipole moments of TN and the $j$th RN. $J_j(\lambda)$ is the overlap between the emission spectrum of the donor and the absorption spectrum of $A_j$. $R_j$ and $J_j(\lambda)$, as well as $n$, are assumed to be constant during the communication. $\kappa_{j,i}$ is the relative orientation factor of the donor and $A_j$ during the generation and relaxation of the exciton $i$. For isotropically free molecules, $\kappa_{j,1}^2, \ldots, \kappa_{j,N}^2$, as well as $\kappa_{1,i}^2, \ldots, \kappa_{k,i}^2$ are i.i.d. random variables with the probability distribution defined in (7).

At time $T_{g,i} + \tau_{DA,i}$, the exciton $i$ is either removed from the system by the fluorescence of TN, or is transferred to one of the

RNs. The probability of the transfer for the $i$th exciton to $A_j$ in terms of process rates is given as

$$P_{\mathrm{FRET},j,i} = \frac{k_{T,j,i}\mathbf{1}_{r,j,i}}{k_R + \sum_{l=1}^{k} k_{T,l,i}\mathbf{1}_{r,l,i}} \tag{19}$$

where $\mathbf{1}_{r,j,i} = 1$ when $A_j$ is available at time $T_{r,i}$, and $\mathbf{1}_{r,j,i} = 0$ when $A_j$ is excited at time $T_{r,i}$.

The transmission of bit-1 is simulated following a Monte Carlo approach. We numerically obtain $p_{1,j}$, and then, investigate the broadcast channel capacity and ISI probability in Section V-B.

## IV. Information Routing in FRET-Based Nanonetworks

The ability of controlling the route of the information flow in a nanonetwork comprising many nanonodes with various sensing, computing and actuating capabilities brings the advantage of making the nanonodes cooperatively perform several complex tasks. In this section, we propose electrically and chemically active routing mechanisms to control the information flow in an FRET-based nanonetwork exploiting the remarkable dependence of FRET on spectral and spatial parameters of fluorophores.

### A. Electrical Routing

Semiconductor nanoparticles are extensively used in fluorescence-based applications owing to their exceptional properties which are mainly originated from the effect of quantum confinement, such as size-dependent tunable emission, high quantum yield and broad absorption spectrum as well as narrowband emission [24]. Another distinctive property of semiconductor nanoparticles is Quantum Confined Stark Effect (QCSE) that defines the Stark Shift in the emission spectrum of the particle with varying internal or external electric field [25]. QCSE brings another dimension to the spectral tunability of the emission allowing post-synthesis tuning of the optical characteristics.

In a quantitative sense, the shift of a semiconductor nanoparticle in terms of electric field is approximated as a sum of linear and quadratic functions [25] as

$$\Delta E = \mu\xi + \frac{1}{2}\alpha\xi^2 + \dots \tag{20}$$

where $\Delta E$ is the shift in the energy spectrum; $\mu$ is the projection of excited-state dipole; $\alpha$ is the polarizability along the electric field, and $\xi$ is the magnitude of the applied electric field.

The tunability of the emission with an electric field is exploited as a control mechanism over the FRET efficiency in [26]. Becker *et al.* investigate the FRET between CdSe/CdS Quantum Rods (QR) and Cy5-derivative dye molecules exposed to an external electric field, and the switch behavior of the mechanism over FRET is experimentally demonstrated for cryogenic temperatures, i.e., at very low temperatures, obtaining a typical 10 nm wavelength shift [26]. At cryogenic temperatures, the inhomogeneous broadening observed in the molecules' emission and absorption spectra are removed, and thus, the spectrum of single fluorescent molecules becomes very narrower such that the typical spectral shifts (0–20 nm) resultant from the QCSE become comparable to the spectral overlap between the molecules. The idea of electrical control

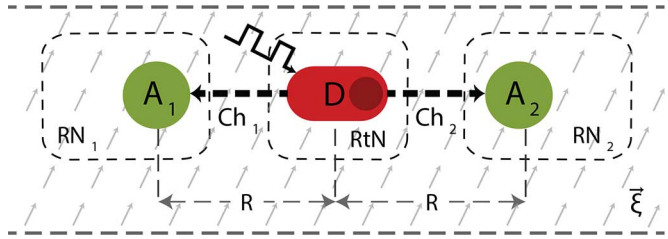


Fig. 3. Demonstration of electrically controllable routing of the communication between a single RtN and two RNs.

over FRET is based on tuning the degree of the spectral overlap between donor CdSe/CdS and acceptor Cy5 by altering the magnitude of the applied electric field. As the electric field increases, the emission spectrum of CdSe/CdS is red-shifted, however, the absorption spectrum of the dye molecule is not affected by the electric field. Thus, the overlap either increases or decreases depending on the relative positions of the emission and absorption spectra of CdSe/CdS and Cy5, respectively. As a result, efficiency is tuned with electric field.

In this study, we further develop the idea introduced in [26] by approaching from the communication perspective and exploiting QCSE in order to enable a nanoscale communication network which is capable of altering its state depending on the magnitude of the applied electric field. Using a semiconductor nanoparticle as a network node brings the selective routing capability to the node such that it becomes able to route the incoming information packets from IS or a preceding node, through one of the FRET channels making the selection according to the magnitude of the applied electric field. Employing this type of routing mechanism brings the advantage of directing the information flow at nanoscale by controlling it at macroscale.

In the considered scenario, a single quantum rod CdSe/CdS as the Router Nanonode (RtN) is the first destination of the information coming from an IS. Two spectrally distinct acceptors as RNs with different absorption characteristics are located in the opposite sides of RtN with a distance $R$ to RtN as demonstrated in Fig. 3.

In order to investigate the performance of the routing mechanism in terms of communication capacity, we approximate the normalized emission of the router CdSe/CdS, i.e., $f_D(\lambda)$, and the absorption spectra of the RN dye molecules, i.e., $\epsilon_{A_1}(\lambda)$ and $\epsilon_{A_2}(\lambda)$, as Gaussian distributions given as

$$f(\lambda) = \exp(k(\lambda - \lambda_c)^2) \tag{21}$$

where $\lambda_c$ is the center wavelength at which emission or absorption is maximum, and $k$ is the fitting parameter which gives the measure of the spectral broadening about the mean wavelength, i.e., linewidth of the spectrum. For a single CdSe/CdS, $\lambda_c$ is 605 nm under zero electric field condition and it is shifted in the red direction with the application of an electric field, thus, $\lambda_{c,\mathrm{CdSe/CdS}}$ is equal to $605+\Delta\lambda$ nm, where $\Delta\lambda$ is the amount of the spectral shift in nanometers. $k$ is set according to the spectral linewidth 1.6 nm of CdSe/CdS at 50 K [26]. At the same cryogenic temperatures, the vibrational broadening of the emission spectrum of single dye molecules is frozen out, and spectral linewidth becomes very narrow compared to the spectrum

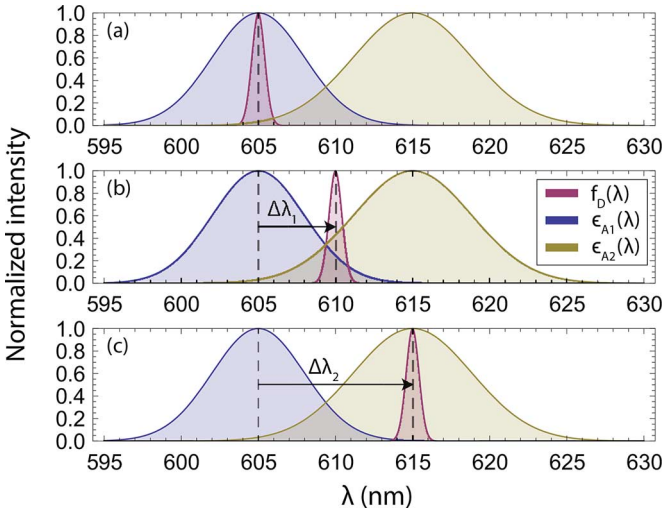


Fig. 4. Approximated emission spectrum of single CdSe/CdS and absorption spectra of the hypothetical dye molecules at different spectral shifts: (a) $\Delta\lambda_0 = 0$, (b) $\Delta\lambda_1 = 5$ nm, (c) $\Delta\lambda_2 = 10$ nm.

of dye's bulk solution. However, the absorption spectra of single dye molecules, which we need to approximate, cannot be measured directly. Fortunately, the emission spectrum of a dye sets an upper limit for the absorption spectrum's linewidth. Based on this, and in parallel to assumptions in [26], the absorption spectra of the dye molecules $A_1$ and $A_2$ are designed hypothetically with $\lambda_{c,A_1} = 605$ nm, $\lambda_{c,A_2} = 645$ nm and linewidths equal to 7 nm and 9 nm, respectively.

The approximated emission spectrum of CdSe/CdS and the absorption spectra of hypothetical dye molecules for different spectral shifts are demonstrated in Fig. 4. Under zero electric field condition, the spectral shift of CdSe/CdS is also zero and $A_1$ and CdSe/CdS have a significant spectral overlap, however, the overlap of $A_2$ and CdSe/CdS is negligible. As the spectral shift increases with increasing electric field, the spectral overlap of CdSe/CdS and $A_1$ decreases with increasing spectral shift; conversely, the spectral overlap of CdSe/CdS and $A_2$ increases. The Förster radius is related to the spectral overlap as follows

$$R_0^6 \propto \int_0^\infty F_D(\lambda)\epsilon_A(\lambda)\lambda^4 \mathrm{d}\lambda \tag{22}$$

As a consequence, $p_1$ and spectral overlap vary proportionally. We analyze the resultant deviation of the capacity for each channel with varying spectral shift in Section V-C.

### B. Chemical Routing

Mimicking the macroscopic machine-like actuating capabilities on the molecular scale is of great interest for nanotechnology. For this aim several artificial molecular machines inspired by the nature, e.g., charge separation in photosynthesis or muscle movement, have been designed [27]. Mechanically interlocked molecules providing controllable and reversible motion can be considered as the most simplest molecular machines with the electrochemically or photochemically active components that undergo basic translational or rotational movements [28]. Here, we focus on a specific kind of synthetic interlocked

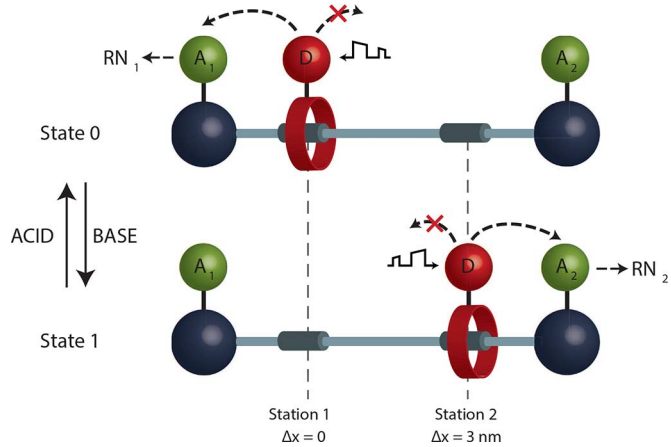


Fig. 5. Demonstration of chemically controllable routing.

molecules, namely [2]rotaxane, that can be employed for selective routing of information in an FRET-based communication network.

[2]rotaxane is an interlocked supramolecule consisting of a macrocyclic ring trapped onto a dumbbell component containing two separate recognition sites and two stopper molecules at the both end of the dumbbell as seen in Fig. 5. The ring undergoes a reversible translational movement between two recognition sites on the dumbbell axes when [2]rotaxane is induced by a chemical or optical signal [28], [29]. Therefore, the ring acts as a bistable molecular shuttle between two stations. There are several studies which combine the ring displacement in [2]rotaxane and the strong distance dependence of FRET in order to develop a mechanical switch that outputs an optical signal. Some of the studies concerning FRET and [2]rotaxane follow a way through replacing the [2]rotaxane components with photoactive molecules [30], and some of them covalently binding the fluorophores onto the ring and stopper components [31]. In both ways, the fluorescence intensity of the donor molecule located at the end of the axis is altered when the ring acting as acceptor or bearing an acceptor molecule is moving through the axis.

In our proposed model, two acceptor fluorophores of the same kind as the receiver nanonodes are immobilized through covalent binding on the stoppers of a chemically active [2]rotaxane, and a donor fluorophore as the routing node, i.e., RtN, is covalently bound to the macrocycle DB24C6 [29] as demonstrated in Fig. 5. The length of the [2]rotaxane axis is assumed to be 5 nm. The recognition sites consist of dialkylammonium center and 4,4′-bipyridinium unit as in the configuration proposed in [29]. The recognition sites are assumed to be located at 1 nm inside from the stopper molecules. The center of the transition dipole moments of the donor and acceptor molecules are assumed to be aligned linearly on a second axis parallel to the [2]rotaxane axis. The donor molecule on the ring is the first destination of the information coming from IS. In the stable case, i.e., state 0, the macrocycle with the donor molecule is expected to be located around the dialkylammonium center because of the strong hydrogen bonding interactions between the cycle and the center. Upon the protonation, the macrocycle moves from the ammonium station to the bipyridinium station and is located around it, therefore, the system goes into state 1 [29]. The reversible

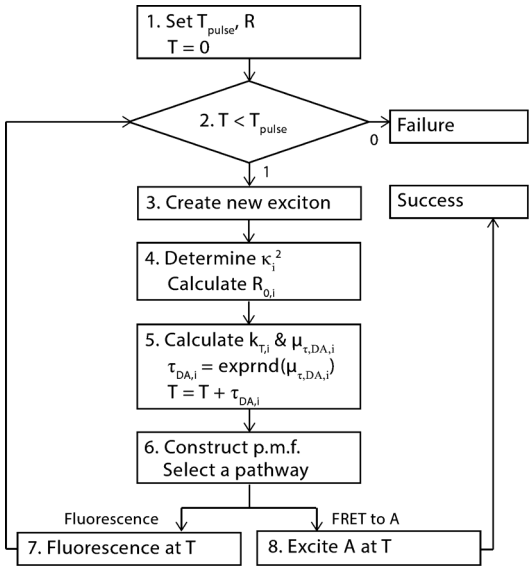


Fig. 6. Monte Carlo algorithm for the simulation of the transmission of bit-1 through the point-to-point communication channel.

displacement of the macrocycle is based on an electrochemical stimuli such as acid/base treatment [29]. We do not go into detail about the chemical reactions, but analyze the effect of ring displacement on the capacity of the channels established among three nodes located on the [2]rotaxane system in Section V-D.

## V. Information Theoretical Analysis

In this section, we investigate the performance of FRET-based point-to-point and broadcast communications in terms of information theoretical capacity and ISI probability for varying system parameters. Furthermore, we simulate the electrical and chemical routing scenarios, and derive the channel capacity for each state of the routers in order to evaluate the performance of each routing scheme.

### *A. Analysis of FRET-Based Point-to-Point Communications With Multi-Exciton Transmission*

The degree of randomness over the transmission probability of bit-1 makes it hard to find an analytical expression for the information theoretical capacity of the channel. Therefore, we simulate the channel model for the transmission of bit-1 following a Monte Carlo approach.

*1) Simulation Algorithm:* Fig. 6 demonstrates the algorithm used in the simulations operating through the following steps:

1) The pulse length $T_{\rm pulse}$ and the internodal distance $R$ between TN and RN are set. The simulation time $T$ is set to its initial value 0.
2) The algorithm checks whether simulation time reaches at $T_{\rm pulse}$.
3) If $T_{\rm pulse}$ is not reached, a new exciton is generated on donor, i.e., TN, with the index $i$ at time $T = T_{g,i}$. If $T > T_{\rm pulse}$, then the simulation ends with the failure of the transmission of bit-1.
4) For the time that the new exciton is created, the relative orientation of the isotropically free molecules is determined randomly according to the distribution (7). The Förster radius $R_{0,i}$ between the donor and the acceptor for the $i$th exciton is calculated accordingly.
5) FRET rate $k_{T,i}$ is determined using $R_{0,i}$. The algorithm checks the availability of the acceptor at $T = T_{g,i}$, and calculates mean lifetime $\mu_\tau$ accordingly. The lifetime $\tau_{DA}$ is determined randomly from the exponential distribution with mean $\mu_\tau$. The simulation time $T$ is proceeded as $\tau_{DA}$, i.e., $T = T_{r,i}$, since it is not possible for another exciton to be generated until the donor relaxes.
6) At time $T = T_{r,i}$, the algorithm checks the availability of the acceptor, and calculates $P_{{\rm FRET},i}$ using the relation (15). A probability mass function (p.m.f.) for the possible pathways is constructed. The pathway that will be followed by the exciton $i$ is selected randomly according to the constructed p.m.f.
7) In the case that the exciton undergoes fluorescence, the donor is relaxed through fluorescence at $T = T_{r,i}$, and the exciton $i$ is removed from the system. The simulation continues at Step 2.
8) In the case that the exciton is transferred to RN through FRET, the donor is relaxed, and the acceptor is excited at time $T = T_{r,i}$. Therefore, the simulation ends with the successful transmission of bit-1.

The simulation is carried out for two hypothetical molecules with the typical parameters; $\tau_D = 2$ ns, $\tau_A = 2$ ns, and $R_0 = 5$ nm for the mean orientation factor [9], and with varying $T_{\rm pulse}$ and $R$. $p_1$ is calculated as the number of the successful transmissions divided by the total number of the simulation runs. Note that the simulation is repeated until $p_1$ converges to a finite value.

*2) Channel Capacity:* The channel capacity $C$ is derived information theoretically from the obtained value of $p_1$, given that $p_0 = 1$ in all of the cases. Since the transmission of bit-0 is always successful and the transmission of bit-1 is problematic, the channel information theoretically shows Z-channel characteristics [32]. The channel capacity of Z-channel for each parameter is derived as the maximum mutual information between input and output alphabets over all input distributions. By omitting the calculations, the results are demonstrated in Fig. 7. As expected, the capacity significantly decreases with increasing $R$ after a critical distance due to the sixth power dependence of the $P_{\rm FRET}$ on $R$. For low values of $T_{\rm pulse}$, the critical distance is approximately equal to $R_0$. However, as $T_{\rm pulse}$ increases, the number of excitons employed in the transmission of bit-1 increases, therefore, the capacity is considerably improved over internodal distances larger than $R_0$.

*3) ISI and Achievable Rates:* If the bit period $T_b$ is not set carefully, the resultant communication might be ambiguous, such that, the excitons created during $T_b$ might arrive the RN at a time greater than $T_b$, i.e., in the next bit interval. Since the governing time parameters are exponential random variables, it is not possible to completely remove ISI, however, the ISI probability might be reduced to negligible values by setting $T_b$ over some threshold value. In order to determine the ISI probabilities for varying $T_b$, we observe the maximum removal times of the excitons that reaches to RN conducting the Monte Carlo simulations and recording the time data for the last-arrive

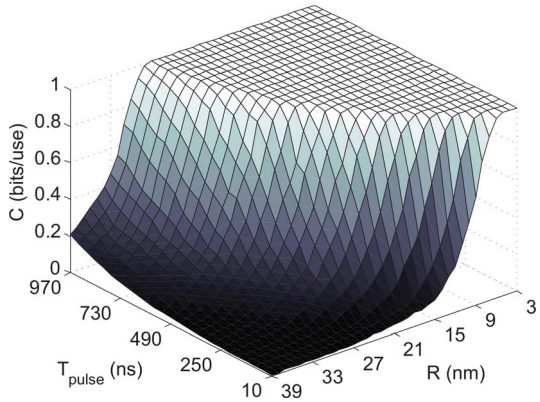


Fig. 7. Channel capacity with varying $T_{\rm pulse}$ and $R$.

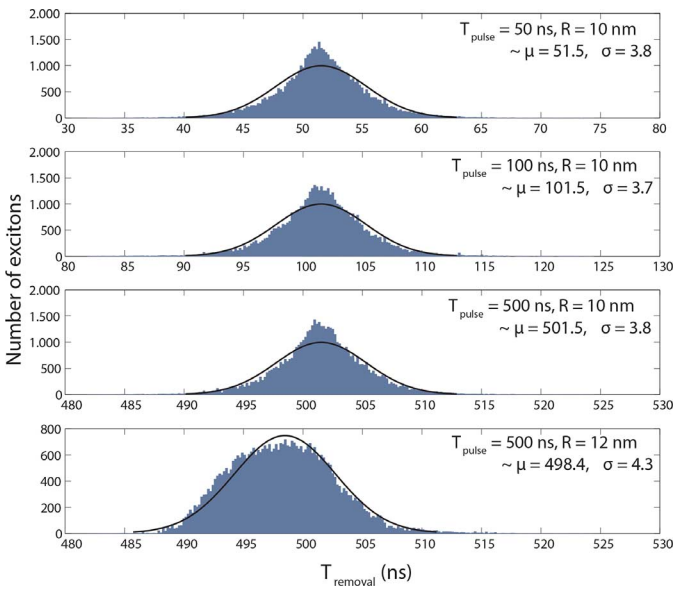


Fig. 8. Removal times with Gaussian fit for different $T_{\rm pulse}$ and $R$.

excitons. The histograms of the obtained data are demonstrated in Fig. 8 for four different typical combinations of $T_{\rm pulse}$ and $R$ with Gaussian fits. According to the data, we conclude that, for the same $R$, varying $T_{\rm pulse}$ only changes the mean of the distribution of the removal times in proportion, and the variance of the removal times is not affected considerably. However, for constant $T_{\rm pulse}$, varying $R$ results in a significant variation of the distribution of the removal times. This is due the fact that the variation in $T_{\rm pulse}$ has no effect on the excited state lifetimes of the molecules, however, the variation in $R$ alters the process rates significantly, and finally results in the variation of the time parameters. Therefore, ISI probabilities are analyzed for a constant $T_{\rm pulse}$ and varying $R$. Setting $T_{\rm pulse} = 10$ ns and $T_b = T_{\rm pulse} + T_{\rm off}$, the resultant ISI probabilities for varying $R$ are demonstrated in Fig. 9. ISI considerably decreases with increasing $R$ for different values of $T_{\rm off}$, and setting $T_b$ as greater than $T_{\rm pulse} + 20$ ns results in negligible ISI for all $R$ values.

The upper bound for reliable communication rate can be expressed by $R_{\max} = C/T_b$. Neglecting ISI by setting $T_{\rm off} = 20$ ns, the achievable rate for different pulse lengths over varying internodal distances is shown in Fig. 10. We conclude that nanomachines can reliably communicate at a

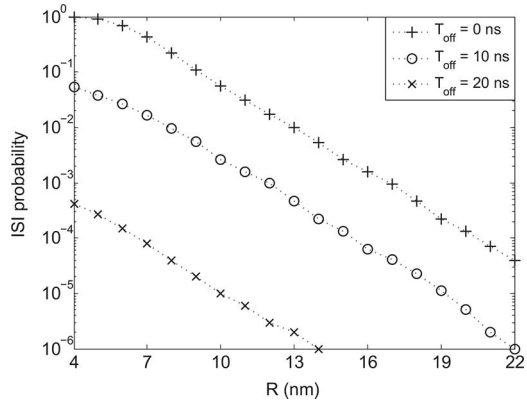


Fig. 9. ISI probability for several $T_{\rm off}$ with varying $R$.

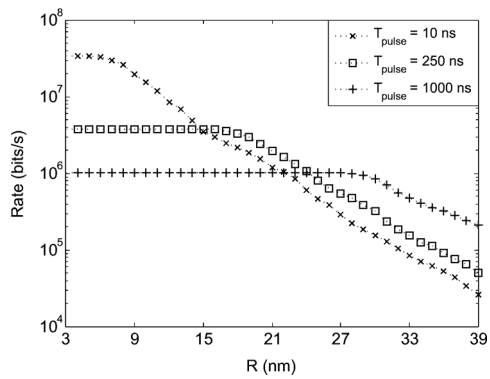


Fig. 10. Achievable rates for several $T_{\rm pulse}$ with varying $R$.

rate up to 33 Mbps over 5-nm distance, and at a rate up to 300 kbps over 35-nm distance. Note that, for short-range communication, using shorter pulses results in higher data rates, however, over longer distances, we can get higher data rates with long-width pulses. With these results, we can certainly conclude that FRET-based communication strongly outperforms other molecular communication methods by means of communication rate.

### *B. Analysis of FRET-Based Broadcast Communications With Multi-Exciton Transmission*

In this section, we analyze the information theoretical capacity and investigate the ISI problem for FRET-based broadcast communication channel of which principles are expressed in Section III-B. The transmission of bit-1 from TN to the $m$th RN out of $k$ RNs through the broadcast channel is simulated using the algorithm described in Fig. 11. The transmission probability of bit-1 between TN and the $m$th RN, i.e., $p_{1,m}$, is obtained following a Monte Carlo approach. The algorithm used for broadcast communication differs from the single pair communication algorithm basically in Step 9 and Step 10, such that the simulation does not end in success until the $m$th RN is excited. If $j$th RN with $j \neq m$ is excited, the simulation continues with Step 10, where the $i$th exciton on the $j$th RN is removed by fluorescence after a random occupation time.

In the simulations, we assume all of the RNs have the same optical characteristics and are at the same distance $R$ from TN. We employ the same hypothetical molecules as in Section III-A, with the typical values of the intrinsic parameters, such that,

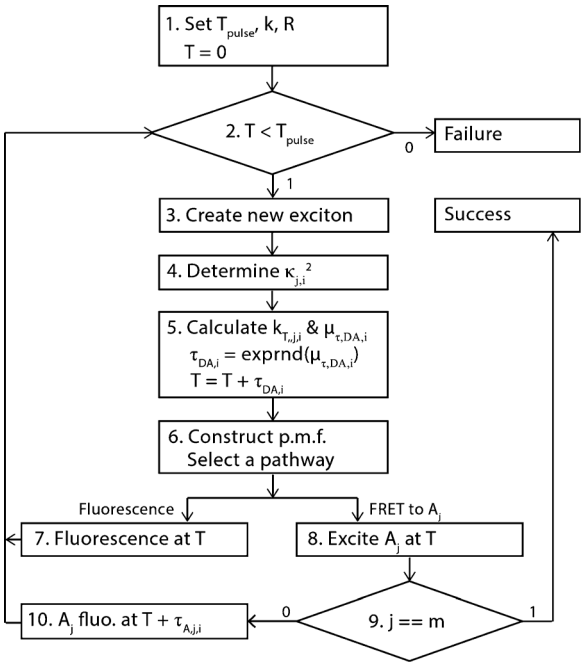


Fig. 11. Monte Carlo algorithm for the simulation of the transmission of bit-1 through the broadcast communication channel.

$\tau_D = 2$ ns, $\tau_A = 2$ ns and $R_0 = 5$ nm for the mean relative orientation [9]. $p_{1,m}$ is calculated as the proportion of the number of successful transmissions of bit-1 from TN to the $m$th RN over the total number of simulation runs, and the simulation is repeated until $p_{1,m}$ converges. The information theoretical capacity of the resultant Z-channel is determined as the maximum mutual information between the input and output alphabets over all input distributions [32]. The derived capacity of the channel between TN and $m$th RN gives the capacity of the overall broadcast communication channel.

*1) Channel Capacity:* The obtained capacity values for typical $k$, $R$ and $T_{\rm pulse}$ combinations are plotted in Fig. 12. A remarkable result of the analysis is that the critical distance where the capacity begins to significantly decrease does not alter notably with varying number of RNs if $T_{\rm pulse}$ is set sufficiently large. Therefore, the capacity of point-to-point communication channel can be achieved in a broadcast network with appropriately selected pulse lengths. However, for low values of $T_{\rm pulse}$, addition of extra RNs into the network reduces the capacity for the same internodal distances, since the number of excitons generated with a short pulse might not be sufficient to excite all of RNs. Furthermore, we observe that the slope of the capacity decrease for distances greater than the critical distance is sharpened as $k$ increases. This is because as the number of RNs increases, the FRET processes that contribute to the relaxation of the donor increases. As a result, the sixth power dependence of many FRET processes combine improving the distance effect on the capacity expression.

*2) ISI and Achievable Rates:* The ISI probability is analyzed using the last exciton removal times on the acceptor, and we conclude that the distribution of the removal times does not alter notably for varying $T_{\rm pulse}$, however, the variation of $R$ significantly effects the characteristics of the distribution as in the case of point-to-point communications. By setting $T_{\rm pulse} = 10$ ns

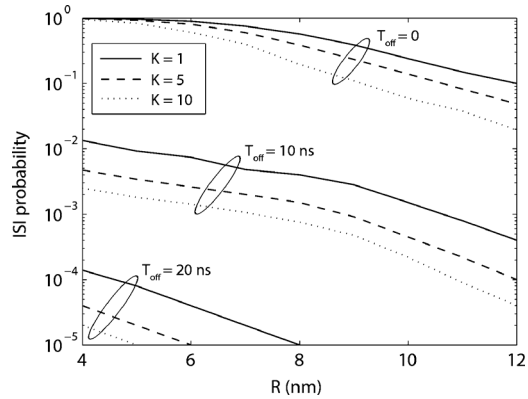


Fig. 12. Broadcast channel capacity for several $k$ with varying $T_{\rm pulse}$ and $R$. (a) $k = 2$, (b) $k = 5$, (c) $k = 10$.

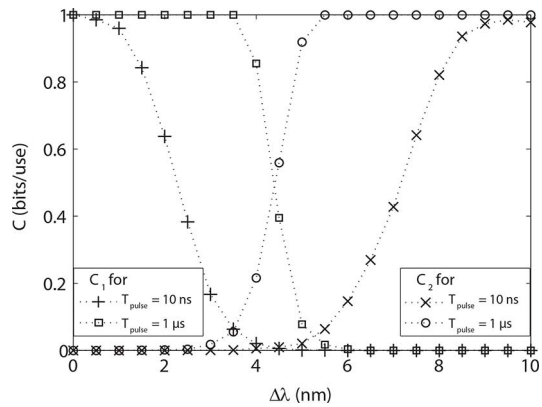


Fig. 13. ISI probability of broadcast communication for different $k$ and $T_{\rm off}$ with varying $R$.

and $T_b = T_{\rm pulse} + T_{\rm off}$, the result of the analysis is plotted for different combinations of $k$, $R$ and $T_{\rm off}$ in Fig. 13. As is seen, the ISI probability decreases with increasing $R$ and the increasing number of RNs. Setting the offset time as $T_{\rm off} = 20$ ns results in a negligible probability of ISI as in the point-to-point communications. Therefore, the achievable rates for broadcast communication are approximately the same as that of the point-to-point communication with sufficiently large $T_{\rm pulse}$.

### C. Analysis of Electrical Routing

The performance of the electrical routing scheme for the nanonetwork demonstrated in Fig. 3 is analyzed information theoretically in terms of communication capacity. We assume that bit-1 is represented with a pulse of duration $T_{\rm pulse}$, and bit-0 is represented as silence during a time slot of duration $T_b$ which is assumed to be long enough to overcome ISI. The distance of RtN to both RNs is set to $R_{0,DA_1}$ which is the Förster radius of CdSe/CdS-$A_1$ pair when the electric field is zero. The molecules on the nanomachines are assumed to be isotropically free, therefore orientation factor $\kappa^2$ has the probability distribution defined in (7) independently for each exciton. The configuration is similar to that of the broadcast communication investigated in Section III-B except that $R_0$ changes also with varying spectral shift. The transmission probability of bit-1 through the individual channels, i.e., channel RtN-$RN_1$ and RtN-$RN_2$, for varying spectral shift is obtained using the broadcast simulation algorithm described in Fig. 6 and following a Monte Carlo approach. The varying channel

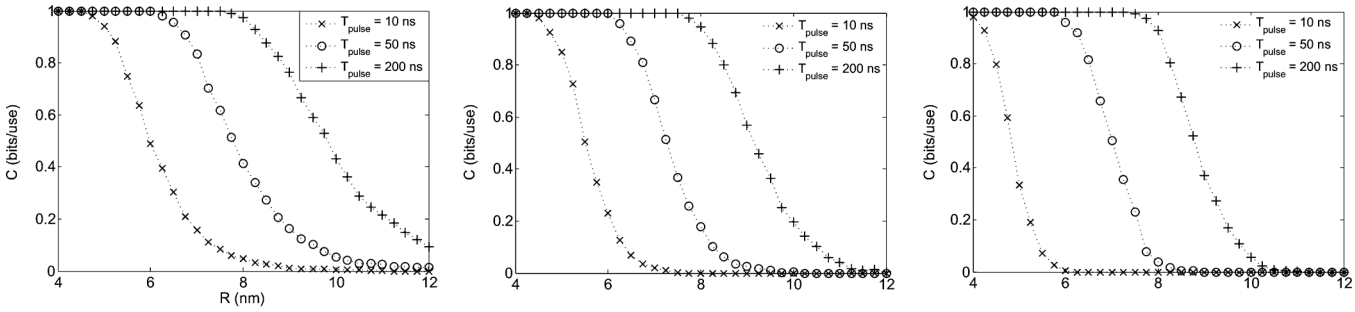


Fig. 14. Channel capacity of individual channels, i.e., $C_1$ and $C_2$ for varying spectral shift $\Delta\lambda$.

capacity is then derived using the obtained value of $p_1$ for both channels.

The resultant capacity for different pulse lengths and varying level of wavelength shift is plotted in Fig. 14. As is seen for each value of $T_{\text{pulse}}$, RtN-$\text{RN}_1$ channel capacity is maximum under zero electric field condition and decreases to negligible values with increasing shift; conversely, RtN-$\text{RN}_2$ channel capacity is negligible at zero electric field, however, it increases to its maximum as shift increases to 10 nm. Therefore, around the zero electric field, the information is transmitted only to $\text{RN}_1$; conversely, RtN transmits only to $\text{RN}_2$, when the shift is around 10 nm. Additionally, we conclude that increasing $T_{\text{pulse}}$ decreases the wavelength shift required for full switching between two channels, therefore, larger $T_{\text{pulse}}$ provides faster routing performance.

### D. Analysis of Chemical Routing

In order to investigate the performance of the chemical routing method proposed in Section IV-B, we analyze the deviation of the communication capacity of the channels RtN-$\text{RN}_1$ and RtN-$\text{RN}_2$ with varying position of the ring. The transition probability of bit-1 through the individual communication channels is simulated using the broadcast simulation algorithm described in Fig. 11. Here, we assume the transition dipole moments of the molecules are in-line with the secondary axis, the relative orientation factor is deterministic with $\kappa^2 = 4$. The Förster radius of the donor-acceptor pairs $R_0$ is assumed to be 2 nm for in-line orientation and constant during the transmission of the information bits. Although the relative orientation factor is maximized, $R_0$ is taken as relatively small in order to show that one can pick the donor and acceptor pair from a large set of fluorophores which are not required to have significant spectral similarity [9]. Bit-1 is represented with a $T_{\text{pulse}}$-duration optical pulse coming from IS at the beginning of a time slot with duration $T_b$ that is assumed to be enough for avoiding ISI, and bit-0 is represented as silence during the time slot. We assume that the effective volume of the laser beam uniformly covers the whole trajectory traveled by the donor molecule, such that, the donor is excited with the same probability at each point that it is located. The transmission probabilities of bit-1, i.e., $p_1$, for the individual channels are calculated as the number of successful transmissions divided by the total number of simulations.

Using the obtained $p_1$ values, and given $p_0 = 1$, the information theoretical capacities of the individual channels are calculated for different locations of the donor, i.e., the ring. The results are plotted for two different $T_{\text{pulse}}$ values in Fig. 15. As is seen in the figure, when the ring is at its initial position, i.e., $\Delta x = 0$, RtN transmits the incoming information only to $\text{RN}_1$ with the capacity $C_1 = 1$ bit/use. At this position, the channel RtN-$\text{RN}_2$ is in the closed state with $C_2 = 0$, such that, $\text{RN}_2$ cannot receive any information from RtN. As with the protonation, the macrocycle slightly moves in the direction of station 2, and $C_2$ increases while $C_1$ decreases with about sixth degree dependence on the displacement. If the communication is established when the displacement of the macrocycle is around 1.5 nm, both channels are in the transition states, and RtN broadcasts the incoming information to both of the RNs in a relatively unreliable manner. When the macrocycle reaches at the station 2, the channel 2 enters into open state with the communication capacity $C_2 = 1$ bits/use, while channel 1 becomes closed. Note that for different $T_{\text{pulse}}$, the displacement required for the transition between two states of the channels does not change significantly, however, the capacity of the broadcast communication in the transition state, i.e., when $\Delta x$ is around 1.5 nm, increases notably for large pulse lengths.

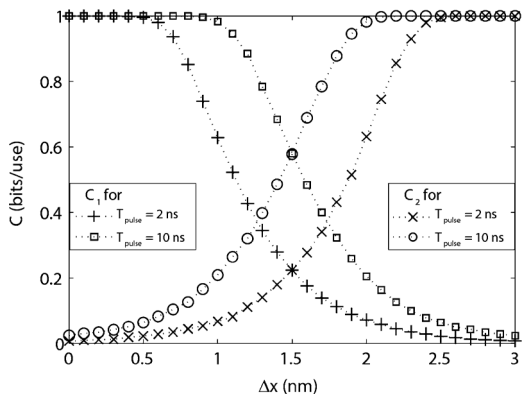


Fig. 15. Channel capacities of individual channels, i.e., $C_1$ and $C_2$, with varying displacement of macrocycle.

## VI. Conclusion

In this study, FRET-based communication is investigated for point-to-point and broadcast cases utilizing multiple excitons as information carrier. The conducted simulations using Monte Carlo algorithms demonstrate that the multi-exciton transmission brings a remarkable performance improvement by means of channel reliability and coverage area, and makes the broadcast communication realizable with notably high channel capacities over the same coverage as in the point-to-point case.

The proposed routing schemes point out the possibility of controlling the route of the information flow in FRET-based nanonetworks by electrical and chemical stimulations. As with the further advances in nanotechnology, we believe that FRET-based nanocommunication and nanonetworking concepts, some of which are proposed in this study, will pave the way for the design of future molecular computers.

## REFERENCES


[1] I. F. Akyildiz, J. M. Jornet, and M. Pierobon, "Nanonetworks: A new frontier in communications," *Commun. ACM*, vol. 54, pp. 84–89, 2011.

[2] I. F. Akyildiz and M. J. Jornet, "Electromagnetic wireless nanosensor networks," *Nano Commun. Netw.*, vol. 1, no. 1, pp. 3–19, 2010.

[3] L. P. Giné and I. F. Akyildiz, "Molecular communication options for long range nanonetworks," *Comput. Netw.*, vol. 53, no. 16, pp. 2753–2766, 2009.

[4] M. Kuscu and O. B. Akan, "A physical channel model and analysis for nanoscale molecular communications with Förster resonance energy transfer (FRET)," *IEEE Trans. Nanotechnol.*, vol. 11, pp. 200–207, 2012.

[5] M. Kuscu and O. B. Akan, "Multi-step FRET-based long-range nanoscale communication channel," *IEEE J. Sel. Areas Commun.*, vol. 31, no. 12, pp. 715–725, 2013.

[6] M. Kuscu and O. B. Akan, "A communication theoretical analysis of FRET-based mobile Ad Hoc molecular nanonetworks," *IEEE Trans. NanoBiosci.*, 2014, to be published.

[7] M. Kuscu and O. B. Akan, "Coverage and throughput analysis for FRET-based mobile molecular sensor/actor nanonetworks," *Nano Commun. Netw.*, vol. 5, no. 1–2, pp. 45–53, 2014.

[8] M. Kuscu and O. B. Akan, "An information-theoretic model and analysis of graphene plasmon-assisted FRET-based nanocommunication channel," in *Proc. ACM NANOCOM*, 2014.

[9] J. R. Lakowicz, *Principles of Fluorescence Spectroscopy*, 3rd ed. Baltimore, MD, USA: Springer-Verlag, 2006.

[10] E. A. Jares-Erijman and T. M. Jovin, "FRET imaging," *Nature Biotechnol.*, vol. 21, pp. 1387–1395, 2003.

[11] L. Stryer, "Fluorescence energy transfer as a spectroscopic ruler," *Annu. Rev. Biochem.*, vol. 47, pp. 819–846, 1978.

[12] P. T. Snee, R. C. Somers, G. Nair, J. P. Zimmer, M. G. Bawendi, and D. G. Nocera, "A ratiometric CdSe/ZnS nanocrystal pH sensor," *J. Amer. Chem. Soc.*, vol. 128, no. 41, pp. 13320–13321, 2006.

[13] Z. Zhou, M. Yu, H. Yang, K. Huang, F. Li, T. Yi, and C. Huang, "FRET-based sensor for imaging chromium(III) in living cells," *Chem. Commun.*, no. 29, pp. 3387–3389, 2008.

[14] A. C. S. Samia, X. Chen, and C. Burda, "Semiconductor quantum dots for photodynamic therapy," *J. Amer. Chem. Soc.*, vol. 125, no. 51, pp. 15736–15737, 2003.

[15] W. R. Dichtel, J. M. Serin, C. Edder, J. M. J. Frechet, M. Matuszewski, L. Tan, T. Y. Ohulchanskyy, and P. N. Prasad, "Singlet oxygen generation via two-photon excited FRET," *J. Amer. Chem. Soc.*, vol. 126, no. 17, pp. 5380–5381, 2004.

[16] S. K. Sekatskii, M. Chergui, and G. Dietler, "Coherent fluorescence resonance energy transfer: Construction of nonlocal multiparticle entangled states and quantum computing," *Europhys. Lett.*, vol. 63, p. 21, 2003.

[17] M. Kuscu, D. Malak, and O. B. Akan, "An information theoretical analysis of broadcast networks and channel routing for FRET-based nanoscale communications," in *Proc. 2nd IEEE MoNaCom*, 2012.

[18] T. Förster, "Zwischenmolekulare energiewanderung und fluoreszenz," *Annalen der Physik*, vol. 437, pp. 55–75, 1948.

[19] D. Badali and C. C. Gradinaru, "The effect of Brownian motion of fluorescent probes on measuring nanoscale distances by Förster resonance energy transfer," *J. Phys. Chem.*, vol. 134, no. 22, p. 225102, 2011.

[20] R. Roy, S. Hohng, and T. Ha, "A practical guide to single-molecule FRET," *Nature Methods*, vol. 5, pp. 507–516, 2008.

[21] S. K. Sekatskii, G. Dietler, and V. S. Letokhov, "Single molecule fluorescence resonance energy transfer scanning near-field optical microscopy," *Chem. Phys. Lett.*, vol. 452, pp. 220–224, 2008.

[22] W. C. W. Chan and S. Nie, "Quantum dot bioconjugates for ultrasensitive nonisotopic detection," *Science*, vol. 281, pp. 2016–2018, 1998.

[23] J. Tisler, R. Reuter, A. Lammle, F. Jelezko, G. Balasubramanian, P. R. Hemmer, F. Reinhard, and J. Wrachtrup, "Highly efficient FRET from a single nitrogen-vacancy center in nanodiamonds to a single organic molecule," *ACS Nano*, vol. 5, no. 10, pp. 7893–7898, 2011.

[24] A. P. Alivisatos, "Semiconductor clusters, nanocrystals, and quantum dots," *Science*, vol. 271, no. 5251, pp. 933–937, 1996.

[25] S. A. Empedocles and M. G. Bawendi, "Quantum-confined stark effect in single CdSe nanocrystallite quantum dots," *Science*, vol. 278, pp. 2114–2117, 1997.

[26] K. Becker, J. M. Lupton, J. Müller, A. L. Rogach, D. V. Talapin, H. Weller, and J. Feldmann, "Electrical control of Förster energy transfer," *Nature Mater.*, vol. 5, pp. 777–781, 2006.

[27] V. Balzani, A. Credi, F. M. Raymo, and J. F. Stoddart, "Artificial molecular machines," *Angew. Chem. Int. Ed.*, vol. 39, no. 19, pp. 3348–3391, 2000.

[28] A. R. Pease, J. O. Jeppesen, J. F. Stoddart, Y. Luo, C. P. Collier, and J. R. Heath, "Switching devices based on interlocked molecules," *Acc. Chem. Res.*, vol. 34, no. 6, pp. 433–444, 2001.

[29] P. R. Ashton, R. Ballardini, V. Balzani, I. Baxter, A. Credi, M. C. T. Fyfe, M. T. Gandolfi, M. Gomez-Lopez, M. Martinez-Diaz, A. Piersanti, N. Spencer, J. F. Stoddart, M. Venturi, A. J. P. White, and D. J. Williams, "Acid-base controllable molecular shuttles," *J. Amer. Chem. Soc.*, vol. 120, no. 46, pp. 11932–11942, 1998.

[30] Y. Li, H. Li, Y. Li, H. Liu, S. Wang, X. He, N. Wang, and D. Zhu, "Energy transfer switching in a bistable molecular machine," *Organic Lett.*, vol. 7, no. 22, pp. 4835–4838, 2005.

[31] H. Onagi and J. Rebek, "Fluorescence resonance energy transfer across a mechanical bond of a rotaxane," *Chem. Commun.*, no. 36, pp. 4604–4606, 2005.

[32] T. M. Cover and J. A. Thomas, *Elements of Information Theory*. New York: Wiley, 1991.


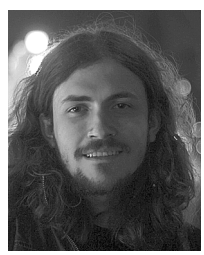

**Murat Kuscu** (S'11) received his B.Sc. degree in electrical and electronics engineering from Middle East Technical University, Ankara, Turkey, in July 2011, and his M.Sc. degree in Electrical and Electronics Engineering Department of Koc University, Istanbul, Turkey, in September 2013. He is currently a research assistant at the Next-generation and Wireless Communications Laboratory and pursuing his Ph.D. degree in electrical and electronics engineering at Koc University, Istanbul, Turkey. His current research interests include nanoscale and molecular communications.

**Ozgur B. Akan** (M'00–SM'07) received his Ph.D. degree in electrical and computer engineering from the Broadband and Wireless Networking Laboratory, School of Electrical and Computer Engineering, Georgia Institute of Technology, Atlanta, GA, USA, in 2004. He is currently a full professor with the Department of Electrical and Electronics Engineering, Koc University, Istanbul, Turkey, and the director of the Next-generation and Wireless Communications Laboratory. His current research interests are in wireless communications, nanoscale and molecular communications, and information theory. He is an Associate Editor of the IEEE TRANSACTIONS ON COMMUNICATIONS, the IEEE TRANSACTIONS ON VEHICULAR TECHNOLOGY, the *International Journal of Communication Systems* (Wiley), *Nano Communication Networks* (Elsevier), and the *European Transactions on Technology*.